

Marek Dudziński*, Andrzej Grządziela*, Marcin Kluczyk*

**NUMERICAL AND EXPERIMENTAL STUDIES
ON THE EFFECT OF DAMAGE
TO A CENTRIFUGAL PUMP CAUSED
BY OWN VIBRATION FREQUENCIES**

ABSTRACT

This article presents a process for developing a simplified model of a centrifugal pump impeller in a CAD environment. Developing a virtual object involved modeling an impeller of a pump both in working condition and with one of the blades damaged. The resonant frequency magnitudes obtained as the result of the analysis of the model were compared with the results obtained in the measurements carried out on a real object. The measurements and simulations were carried out on a pump before and after the damage to the impeller. In order to verify the developed model, particular elements of the model were weighed and then compared with the corresponding masses of the corresponding elements obtained from the virtual object.

Key words:

centrifugal pump, resonance frequencies, numerical calculations.

INTRODUCTION

In this work an impeller used in pump SKA.4.02. was the object of modeling. It is a centrifugal circulating pump with a side annular channel and an open impeller. The most important advantage of this type of pump is its capability of self-suction. However, just like all centrifugal pumps they carry a high risk of cavitation occurring. The phenomenon of cavitation erosion can within a short period of time cause damage to pump elements, including the impeller. The damage can cause changes

* Polish Naval Academy, Faculty of Mechanical and Electrical Engineering, Śmidowicza 69 Str., 81-127 Gdynia, Poland; e-mail: {m.dudzinski; a.grzadziela; m.kluczyk}@amw.gdynia.pl

in the amplitude-frequency characteristics of a pump and under some conditions cause it to work in the range of resonance frequencies. The increased vibration energy transferred to the cast-iron casing in bearing nodes can cause it to crack.

ANALYTICAL CALCULATIONS

Making the model began with initial calculations of resonant frequencies for one blade. The analytical method was used for the calculations. Calculations were also carried out for a blade of reduced height and from this the damage simulation effect was obtained. Parameters used for the calculations were as follows:

1. Geometrical dimensions:

- blade in working condition: thickness 5 [mm],
width 25 [mm],
height 60 [mm].
- damaged blade: thickness 5 [mm],
width 25 [mm],
height 50 [mm].

2. Material particulars:

$$\text{Brass, } E = 115 \cdot 10^9 \text{ [Pa], } \rho = 8500 \left[\frac{\text{kg}}{\text{m}^3} \right].$$

For the own vibration, frequencies (flexural vibrations) are derived from the dependence [1], [6]:

$$\omega_n = (\lambda_n l)^2 \sqrt{\frac{EI}{\rho A l^4}}. \quad (1)$$

For $n = 1$ $\lambda_n l = 1,875$.

λ — slenderness ratio derived from the dependence:

$$\lambda = \frac{l_w}{i_{min}}, \quad (2)$$

where:

$$l_w = \mu l.$$

Adopting $\mu = 2$ for a one-side fixed blade. While the least cutaway inertia radius i_{min} was calculated using the equation:

$$i_{min} = \sqrt{\frac{I_{min}}{A}}, \quad (3)$$

where:

I_{min} — the least main central inertial moment of the cutaway;

A — cutaway area.

After inserting the data to the formulas the results presented in table 1 were obtained. The table also shows the results of the computer-based simulation in CAD. These results are presented in the graphic form in figures 1 and 2.

When the blade is shortened from 60 [mm] do 50 [mm] (17% reduction in mass) the first own vibration frequency increases 1.44 times.

Table 1. The calculation results of own vibration periodicities and frequencies and the modal analysis in CAD

		First blade		Damaged blade	
		calculations	simulation	calculations	Simulation
ω	[rad/s]	5181		7464	
f	[Hz]	825	833	1188	1201

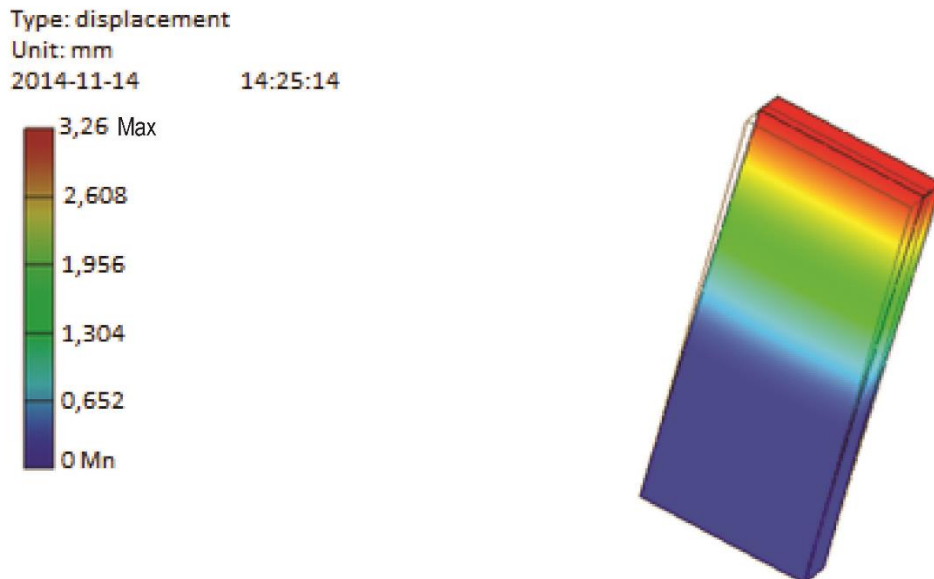


Fig. 1. The modal analysis of the first blade ($f_1 = 833.27$ Hz)

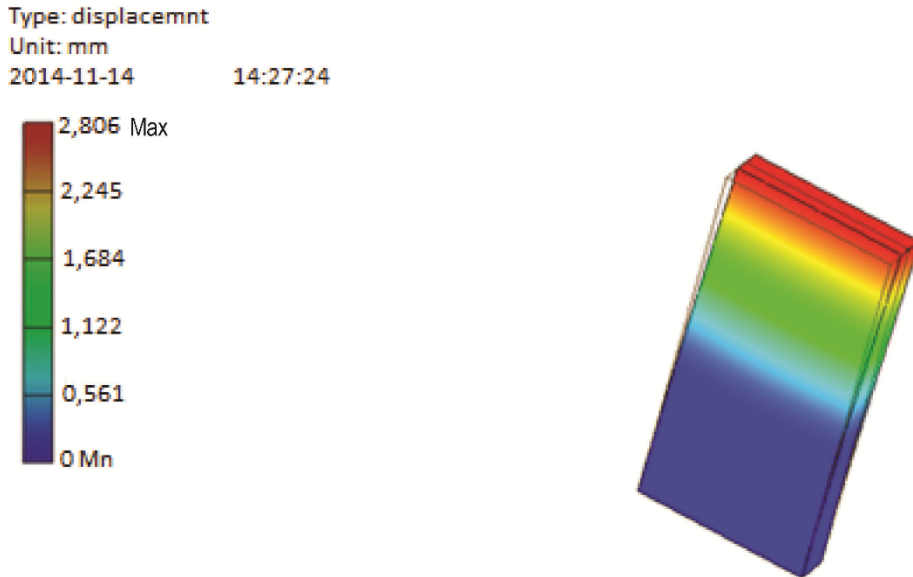


Fig. 2. The modal analysis of the second blade ($f_1 = 1200.85\text{Hz}$)

CALCULATIONS IN CAD

The geometry of the impeller shown in figure 3 went through the process of discretization by means of 15999 linear tetragonal elements, determined by 26918 nodes, which resulted in obtaining the model presented in figure 3.



Fig. 3. The pump impeller used for modeling

Brass having $8.470 \text{ [g/cm}^3\text{]}$ in density was defined for the model. In order to verify the model mass, the impeller was weighed and the results were compared. The purpose was, among others, to verify the correctness of the developed model. The real object mass is 1.884 [kg] . Due to the substantial influence of the distance of the mass from the rotation axis on the mass inertia moment special attention was centered on mapping the shape of blades, especially their elements lying furthest from the rotation axis. It can be assumed that the model was made with a little error equal to 4 [g] , which corresponds to 0.21 [%] error.

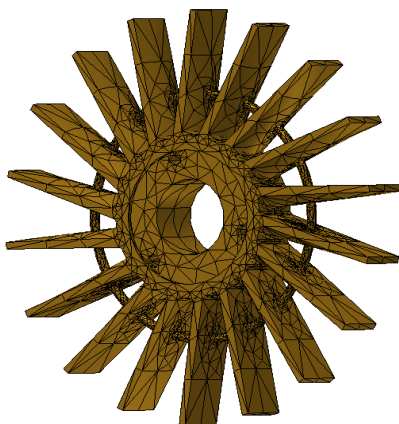
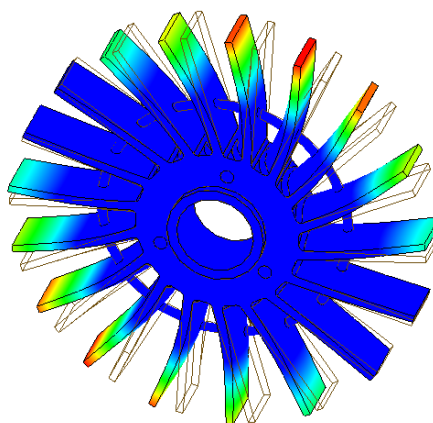


Fig. 4. The discretized impeller model



Rys. 5. An example of the form of impeller own vibrations

The object went through the modal analysis using bolt binding inside the impeller allowing for free rotation — figure 5. The numerical calculations were repeated for the damaged model using the blade shortened by 3 [cm] , and the completely cut off blade. The obtained results of resonant frequencies are presented in table 2.

Table 2. The results of the modal analysis carried out in CAD

	Undamaged model	Damage 3 [cm]	Complete absence of blade
Vibration frquencies	[Hz]	[Hz]	[Hz]
1	1938.67	1914.15	1793.77
2	1939.63	1935.00	1903.95
3	2182.28	2158.83	2036.50
4	2182.31	2160.89	2158.67
5	2331.78	2305.00	2240.75
6	2379.00	2315.84	2347.53
7	2423.79	2428.94	2347.74

EXPERIMENTAL MODAL ANALYSIS

The experimental modal analysis (EMA) is a process involving an experimental determination of resonance frequencies in the investigated system. Using appropriate techniques it is also possible to determine the shape of own vibrations. EMA has several advantages. It is a fast, relatively cheap and simple way of determining resonant frequencies. The initial equation in the modal analysis is the general analysis of a vibration motion [2] (4):

$$m\ddot{x}(t) + c\dot{x}(t) + kx(t) = f(t), \quad (4)$$

where:

m — mass;

c — damping factor;

k — elasticity factor.

Equation (4) can be transformed to the form:

$$[-m\omega^2 + jc\omega + k]X(\omega) = F(\omega). \quad (5)$$

Taking into account the fact that:

$$H(\omega) = \frac{1}{-m\omega^2 + jc\omega + k}. \quad (6)$$

We can write:

$$H(\omega) = \frac{X(\omega)}{F(\omega)}. \quad (7)$$

Magnitude $H(\omega)$ is known as the frequency response function (FRF). FRF describes the relation of Fourier transform at the output from the set $X(\omega)$ to input Fourier transform applied to the set $F(\omega)$. In determining the magnitude of FRF three types of estimator are used $H1$, $H2$ and $H3$. Use of the proper one depends on the expected signal components at the input and the output [5]. The authors used estimator $H3$, proper when noises in both of the signals are at the similar level. Through the use of estimator $H3$ the influence of a noise of the input and output signal on the response results of the frequency set can be minimized. Estimator $H3$ is given by equation [5]:

$$H3 = \sqrt{H1 \cdot H2}. \quad (8)$$

$H1$ is the estimator when the signal at the output has a high magnitude of SNR (signal to noise ratio), $H2$ is the estimator used to minimize the effect of noise of the input signal. Estimators $H1$ and $H2$ are given by (9) and (10).

$$H1 = \frac{G_{XF}}{G_{XX}}. \quad (9)$$

Estimator $H1$ must be interpreted as the relation of the spectrum of mutual signal response and input in the set to the mutual input spectrum [5].

$$H2 = \frac{G_{FF}}{G_{XF}}. \quad (10)$$

Estimator $H2$ is interpreted as the relation of mutual spectrum of the signal input to the spectrum of the mutual input and response. More detailed information concerning the discussed issues are presented in [2], [3], [4], [5], [7].

When discussing the issues concerned with the experimental modal analysis the coherence function can not be omitted. Coherence is a measure whose magnitude is included in the range from 0 to 1 [3]:

$$\gamma_{XF}^2 = \frac{|G_{XF}|^2}{G_{XX}G_{FF}}. \quad (11)$$

In the case of EMA, when coherence between the output and the input signals is 1, it is certain that the response of the set was initiated by the input we recorded during the studies. The coherence magnitudes lower than 1 indicate occurrence of a noise of unknown origin. Still, such signals can be used in further EMA but it is necessary to increase the numbers of averaging. If the coherence magnitude is lower than 0.5 another EMA measurement must be carried out.

MEASUREMENTS OF RESONANT FREQUENCY IN THE PUMP IMPELLER

A measuring set was made to carry out the measurements. It consisted of a hammer weighing 150 g installed with an accelerometer. The same kind of accelerometers were installed in two mutually orthogonal directions on the pump impeller — figure 6. All the signals were synchronized by means of a five-channel measuring cassette B&K 3650-B-120. During the measurements recorded were vibration accelerations in the band from 0.7 Hz to 12.8 Hz. It must be emphasized that for the

input a non-typical solution was used together with a measurement of accelerations, modal hammers available on the market are equipped with sensors. An analysis of the equations (5)–(11) showed that the solution applied will bring the expected results.

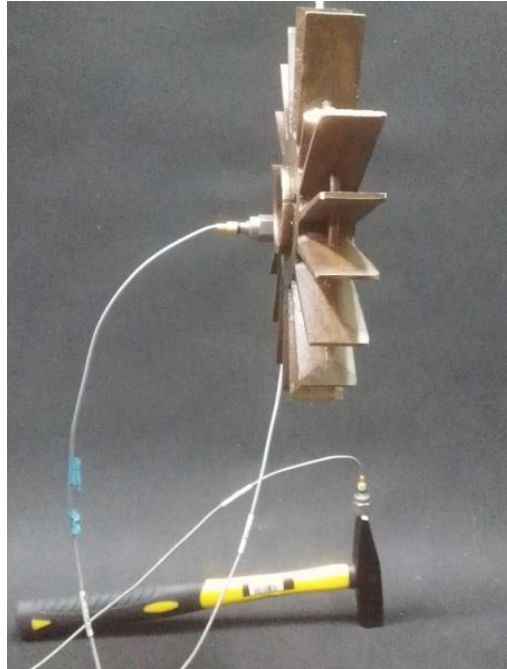


Fig. 6. The measuring set

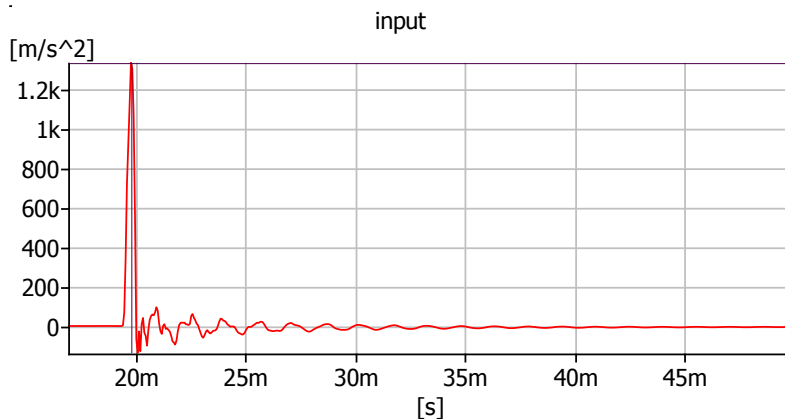


Fig. 7. An example of time distribution of the input

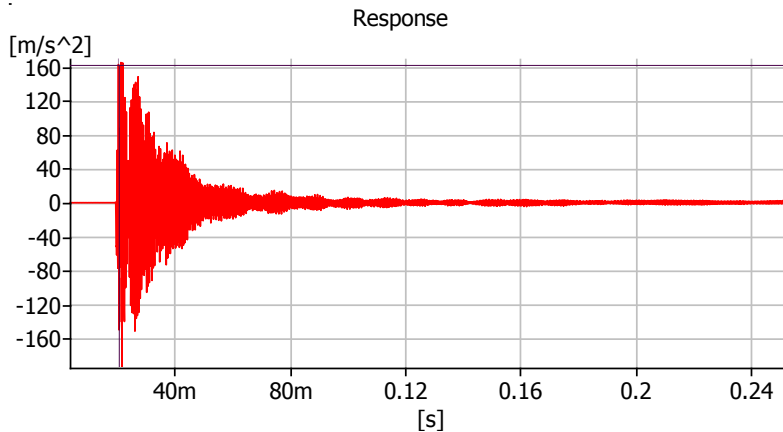


Fig. 8. An example of time distribution of the response recorded on the impeller

In the measurements the distribution of the input and the response to dynamic inputs were recorded — figures 7 and 8. Several measurements were carried out applying impulse actions in various directions. Then they were analyzed using software Pulse LabShop. First the measurements, where in the time distribution of the input more than one significant amplitude was noticed, were rejected. Another stage of the measurements was determining the signal frequency response and input functions. The input signal was always used as the reference signal. The band of analyses, due to the absence of significant amplitudes at higher frequencies, was limited to 6.4 kHz. Further analysis was carried out only with regard to the signals whose coherence magnitude for resonance frequencies were higher than 0.8. In this way obtained were the results presented in table 3 and in figures 9 and 10.

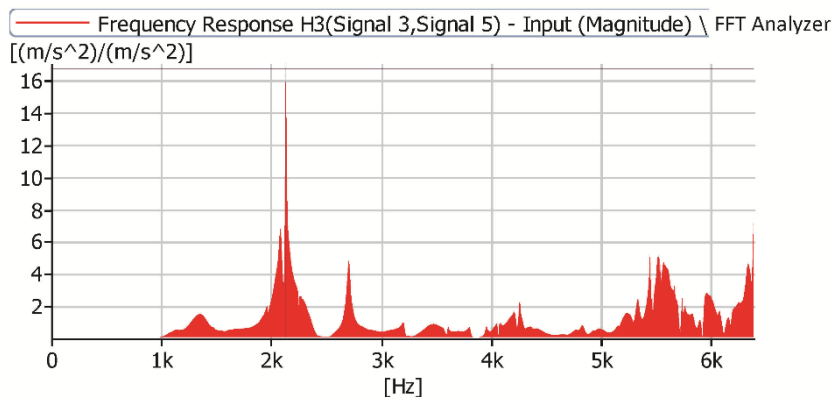


Fig. 9. The frequency response function of the input and response signals in the impeller obtained using $H3$ estimator

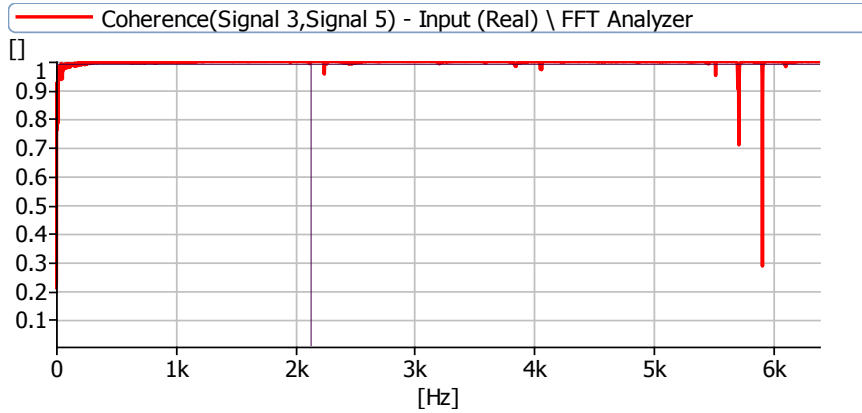


Fig. 10. The coherence function of signals for which FRF is presented in figure 9

In the course of measurements the logical sequence of steps analogue to that from the impeller modeling were repeated. First, signals for undamaged impeller were recorded. The second stage was damaging one of the blades over the length of 3 cm, then one blade was removed. The obtained results of resonance frequencies are presented in table 3.

Table 3. The resonance frequencies recorded during the measurements

	Undamaged impeller		Impeller with damaged blade — 3cm		Impeller without the whole blade	
	Hz	coherence	Hz	coherence	Hz	coherence
1	2074	0.999	2099	0.998	1936	0.991
2	2126	0,993	2188	0,995	2016	0,993

CONCLUSIONS

The model studies and their experimental verification confirm the significant effect of damage to a pump impeller on its resonance frequency. The table presents only two first resonance frequencies recorded in the measurements. They have magnitudes close to the magnitudes obtained in the analysis of the discrete model, which confirms usefulness of the applied experimental modal analysis method.

It must be noted that the way of simulating the loss in mass does not occur in reality as cavitation never damages only one blade without affecting the other ones. Detailed analyses of the effect of cavitation on loss in mass, and as their consequence on changes in resonant frequencies, will be considered in the next publication. The aim

of the investigations will be preparing a methodology for diagnosing impellers in impeller pumps using non-invasive methods. This task can be significant not only for shipbuilding but also for the electric power industry, chemical or petrochemical industries.

REFERENCES

- [1] Czyż W., *Drgania mechaniczne. Mechanika ogólna, cz. IVa, Drgania mechaniczne — teoria drgań*, AMW, Gdynia 1992 [*Mechanical vibrations. General Mechanics, part 4, Mechanical vibrations — theory of vibrations* — available in Polish].
- [2] Deuzkiewicz P., Dobrociński S., Dziurdź J., Flis L., Grządziela A., Pakowski R., Specht C., *Diagnostyka wibroakustyczna okrętowych turbinowych silników spalinyowych*, seria: Biblioteka Problemów Eksploatacji, ITE, Radom 2009 [*Vibro-acoustic diagnostics in marine turbine engines* — available in Polish].
- [3] Gade S., Herlufsen H., *Digital Filter Technique versus FFT Technique for damping measurements*, 'Technical Reviews', 1994, No. 1.
- [4] Gade S., Herlufsen H., Konstantin-Hansen H., *How to Determine the Modal Parameters of Simple Structures*, Brüel & Kjær, Denmark, [online], <http://www.bksv.com/doc/bo0428.pdf>, [access 16.06.2015].
- [5] *Harris' shock and vibration handbook*, 5th edition, ed. C. M. Harris, A. Piersol G., McGraw-Hill, 2002, [online], <http://nguyen.hong.hai.free.fr/EBOOKS/SCIENCE%20AND%20ENGINEERING/MECANIQUE/DYNAMIQUE-VIBRATION/Shock%20&%20Vibration%20Handbook.pdf>, [access 18.06.2015].
- [6] Szturomski B., Flis L. *Wstępna ocena wytrzymałości turbiny elektrowni wodnej z wykorzystaniem komputerowego wspomaganie projektowania*, 'Zeszyty Naukowe AMW', 2006, No. 3, pp. 5–20 [*Preliminary evaluation of water power plant strength using computer supported design* — available in Polish].
- [7] Żółtowski B., *Analiza modalna w diagnozowaniu przekładni zębatej*, 'Diagnostyka', 2000, Vol. 23, pp. 97–101 [*Modal analysis in diagnosing a gear unit* — available in Polish].

NUMERYCZNE I DOŚWIADCZALNE BADANIE WPŁYWU USZKODZEŃ POMPY WIROWEJ NA CZĘSTOTLIWOŚCI DRGAŃ WŁASNYCH

STRESZCZENIE

W artykule zaprezentowano proces tworzenia uproszczonego modelu wirnika pompy wirowej w środowisku oprogramowania CAD. Konstruowanie obiektu wirtualnego obejmowało

modelowanie wirnika pompy sprawnej oraz z symulowanym uszkodzeniem jednej z łopatek. Porównano wyniki częstotliwości rezonansowych uzyskanych w wyniku analizy modelu z uzyskanymi w trakcie pomiarów na rzeczywistym obiekcie. Pomiary i symulacje przeprowadzono na pompie przed i po uszkodzeniu wirnika. W celu weryfikacji sporządzonego modelu poszczególne elementy pompy poddano ważeniu i porównano z masami odpowiednich elementów uzyskanych z obiektu wirtualnego.

Słowa kluczowe:

pompa wirowa, częstotliwości rezonansowe, obliczenia numeryczne.